MOL #78659

Endomorphin-2: a biased agonist at the μ-opioid receptor

Guadalupe Rivero, Javier Llorente, Jamie McPherson, Alex Cooke, Stuart J Mundell, Craig A McArdle, Elizabeth M Rosethorne, Steven J Charlton, Cornelius Krasel, Christopher P Bailey, Graeme Henderson, and Eamonn Kelly

School of Physiology and Pharmacology, University of Bristol, Bristol BS8 1TD, UK (G.R., J.L., J.M., A.C., S.J.M., G.H., E.K.), School of Clinical Sciences, University of Bristol, Bristol BS1 3NY, UK (C.A.M.), Novartis Institutes for Biomedical Research, Horsham, West Sussex, RH12 5AB, UK (E.M.R., S.J.C.), Institut für Pharmakologie & Klin. Pharmazie, Karl-von-Frisch-Strasse 1 35043 Marburg, Germany (C.K.), Department of Pharmacy and Pharmacology, University of Bath, Bath BA2 7AY, UK (C.P.B.)

1

MOL #78659

Running title: *Endomorphin-2 is an arrestin-biased agonist*

Corresponding author: Eamonn Kelly, School of Physiology and Pharmacology, University of

Bristol, University Walk, Bristol BS8 1TD, UK, Tel.: +44 (0)117 3311402; Fax.: +44 (0)117 33

12288; E-mail: E.Kelly@bristol.ac.uk

Number of text pages: 36
Number of tables: 2
Number of figures: 8
Number of references: 39
Number of words in the Abstract: 250
Number of words in the Introduction: 484
Number of words in the Discussion: 1498

Supplemental information – 5 Tables, 4 Figures

Abbreviations: μ opioid receptor (MOPr), [D-Ala2,*N*-MePhe4,Gly-ol]-enkephalin (DAMGO), G

protein-coupled receptor (GPCR), locus coeruleus (LC), G protein-coupled inwardly rectifying K^+

channel current (GIRK), β-funaltrexamine (β-FNA), noradrenaline (NA), Yellow Fluorescent

Protein (YFP), Cyan Fluorescent Protein (CFP), G protein-coupled receptor kinase 2 (GRK2), 6-

monoacetylmorphine (6-MAM), morphine-6-glucuronide (M6G), phosphate buffered saline

(PBS), sodium dodecyl sulphate (SDS), 4',6-diamidino-2-phenylindole dihydrochloride (DAPI).

Abstract

Previously we correlated the efficacy for G protein activation with that for arrestin recruitment for a number of agonists at the μ opioid receptor (MOPr) stably expressed in HEK293 cells (McPherson et al., 2010). We suggested that the endomorphins (endomorphin-1 and -2) may be biased towards arrestin recruitment. In the present study we have investigated this phenomenon in more detail for endomorphin-2, this time using endogenous MOPr in rat brain as well as MOPr stably expressed in HEK293 cells. For MOPr in neurons in brainstem locus coeruleus (LC) slices, the peptide agonists [D-Ala2,N-MePhe4,Gly-ol]-enkephalin (DAMGO) and endomorphin-2 activated inwardly-rectifying K^+ current in a concentration-dependent manner. Analysis of these responses using the operational model of pharmacological agonism confirmed that endomorphin-2 has a much lower operational efficacy for G protein-mediated responses than DAMGO at native MOPr in mature neurons. However endomorphin-2 induced faster desensitization of the K^+ current than DAMGO. In addition, in HEK293 cells stably expressing MOPr, the ability of endomorphin-2 to induce phosphorylation of Ser[375] in the COOH terminus of the receptor, to induce association of arrestin with the receptor, and to induce cell surface loss of receptor was much more efficient than would be predicted from its efficacy for G protein-mediated signalling. Together these results indicate that endomorphin-2 is an arrestin-biased agonist at MOPr and that the reason for this is likely to be the ability of endomorphin-2 to induce greater phosphorylation of MOPr than would be expected from its ability to activate MOPr and induce activation of G protein.

Introduction

Currently there is much interest in the phenomenon of biased agonism, whereby different agonists at a G protein-coupled receptor (GPCR) can induce the receptor to couple to distinct downstream signalling pathways (Reiter et al., 2011; Kenakin 2011). The most likely explanation for biased agonism is that different agonists stabilise distinct active conformations of the GPCR (Kahsai et al., 2011), which couple differentially to downstream signalling pathways. One commonly observed form of biased agonism is that between G protein-dependent and arrestin-dependent signalling (Reiter et al., 2011), although there are likely to be many other variations, such as bias between GPCR coupling to different G protein subtypes. The importance of biased agonism is that ligands could be developed that can selectively activate certain downstream signalling pathways, which has the potential to improve the therapeutic potential to manage a disease and avoid adverse effects.

Agonists at the μ opioid receptor (MOPr) are extremely important drugs for the management of moderate to severe pain (Corbett et al., 2006), but use of these drugs often leads to undesirable effects including respiratory depression, constipation and tolerance, and there is also the potential for abuse (Morgan and Christie 2011). There is therefore a need to develop new analgesic drugs with reduced unwanted effects associated with classical opioids such as morphine (Corbett et al., 2006).

In a recent study we investigated the ability of twenty-two opioid agonists to activate G proteins and recruit arrestin-3 in HEK293 cells stably expressing MOPr (McPherson et al., 2010). We showed that for most of these agonists, there is a strong correlation between these two signalling outputs, however for a few agonists, and particularly the endomorphins, there appeared to be bias towards arrestin recruitment. Since arrestins are implicated in signalling as well as GPCR regulation (Shenoy and Lefkowitz 2011), this could have important consequences for the ability of new ligands based on the endomorphin structure to induce a different array of responses to that of older, morphine-like drugs.

Endomorphin-1 (Tyr-Pro-Trp-Phe-NH$_2$) and endomorphin-2 (Tyr-Pro-Phe-Phe-NH$_2$) are opioid peptides with high affinity and selectivity for the MOPr (Zadina et al., 1997). Although originally identified in extracts from mammalian brain (Zadina et al., 1997) the subsequent inability to identify a precursor protein for either of these peptides has called into question whether they function as endogenous opioids in the mammalian central nervous system (Corbett et al., 2006; Terskiy et al., 2007). However analogues of these peptides have potential as novel analgesic agents and one such drug, Cyt-1010, is reported to be in development (http://www.cytogelpharma.com/news.html).

The purpose of this study was to determine whether endomorphin-2 is a biased agonist at MOPr. Our data indicate that endomorphin-2 is biased towards arrestin recruitment over G protein activation. Furthermore, we show that the likely source for the arrestin bias is the ability of endomorphin-2 to induce greater phosphorylation of MOPr than would be predicted from the ability of this peptide to activate G protein-coupled responses.

Materials and Methods

Drugs: Morphine hydrochloride was from Mcfarlane Smith (Edinburgh UK), etorphine from RTI NIDA (Research Triangle Park, NC) and DAMGO from Bachem AG (Bubendorf, Switzerland). Noradrenaline, β-funaltrexamine (β-FNA), prazosin and cocaine were obtained from Sigma (Gillingham, UK). Endomorphin-2 and chelerythrine were obtained from Tocris (Bristol, UK)

***Brain slice preparation*:** Male Wistar rats (130–170 g) were killed by cervical dislocation, and horizontal brain slices (200–250 µm thick) containing the locus coeruleus (LC) were prepared as described (Bailey et al., 2003). All experiments were performed in accordance with the UK Animals (Scientific Procedures) Act 1986, the European Communities Council Directive 1986 (86/609/EEC) and the University of Bristol ethical review document.

***Whole-cell patch-clamp recordings*:** Slices were submerged in a slice chamber (0.5 ml) mounted on the microscope stage and superfused (2.5–3 ml/min) with artificial cerebrospinal fluid (aCSF) composed of (in mM): NaCl, 126; KCl, 2.5; $MgCl_2$, 1.2; $CaCl_2$, 2.4; NaH_2PO_4, 1.2; D-glucose, 11.1; $NaHCO_3$, 21.4; ascorbic acid, 0.1; saturated with 95% O_2/5% CO_2 at 33–34°C. For patch-clamp recording LC neurons were visualized by Nomarski optics using infrared light and individual cell somata were cleaned by gentle flow of aCSF from a pipette. Whole-cell voltage-clamp recordings (V_h = –60 mV) were made using electrodes (3–6 MΩ) filled with (in mM): K-gluconate, 115; HEPES, 10; EGTA, 11; $MgCl_2$, 2; NaCl, 10; MgATP, 2; Na_2GTP, 0.25 (pH 7.3, osmolarity 270 mOsm). Recordings of whole-cell current were filtered at 2 kHz using an Axopatch 200B amplifier and analysed off-line using pClamp. Activation of MOPrs evoked a transmembrane K^+ current, and by performing whole-cell patch-clamp recordings a real-time index of MOPr activation could be continually recorded. The opioid-evoked current was continuously recorded at a holding potential of –60 mV. MOPrs and $α_2$-adrenoceptors couple to the same set of K^+ channels in LC neurons (North and Williams, 1985). To reduce variation

between cells, the amplitudes of opioid-evoked currents were normalized to the maximum α_2-adrenoceptor mediated current in the same cell evoked by 100 µM noradrenaline (NA) applied in the presence of 1 µM prazosin and 3 µM cocaine.

All drugs were applied in the superfusing solution at known concentrations. Concentration-response curves for MOPr agonists were obtained by cumulative addition. To reduce the influence of desensitization on the slope and maximum of the curves each concentration of drug was added for only 2 min by which time the response had reached a steady state. Each individual cell was exposed to only a limited number of high concentrations ($>EC_{50}$) of the drug and to one supramaximal concentration. The maximum response for each drug obtained in this way was not different from the maximum response observed in other cells exposed to only a single supramaximal concentration of that drug. For example the amplitude of the maximum of the cumulative concentration-response curve for etorphine was 123.0 ± 11.1 % (n=3) that of 100 µM NA, whereas that evoked by a single, maximally effective concentration of etorphine (1 µM) was 142.4 ± 14.3% (n=4) that of 100 µM NA (unpaired t test, p=0.36).

Cell culture: HEK293 cells were maintained at 37°C in 95% O_2, 5% CO_2, in Dulbecco's modified Eagle's medium (Invitrogen, Carlsbad, CA) supplemented with 10% fetal bovine serum, 10 U/ml penicillin, and 10 mg/ml streptomycin. In addition, the culture medium for the HEK293 cells stably expressing MOPr tagged at the NH_2 terminus with HA contained 250 µg/ml G-418 (Geneticin; PAA, Pasching, Austria).

Ser[375] phosphorylation: Agonist-induced phosphorylation of MOPr at Ser[375] was assessed using an IN Cell Analyzer 1000 (GE Healthcare) high content imaging platform as described before with minor variations (Caunt et al., 2010). Cells cultured in 96-well plates were incubated with different concentrations of various MOPr agonists for 10 min at 37°C. Cells were then fixed, permeabilised and immunostained with rabbit anti-pSer[375] polyclonal antibody (1:1,000 dilution,

Cell Signalling Technology, Danvers, MA) followed by incubation with Alexa Fluor 488-conjugated goat anti-rabbit antibody (Life Technologies, Paisley UK), and 4',6-diamidino-2-phenylindole dihydrochloride (DAPI, 600 nM) nuclear stain. Images were acquired and then analyzed with IN Cell Investigator software (Workstation 3.5, GE Healthcare) using a Dual Area Object Analysis algorithm. Fluorescence from DAPI staining was used to define the nuclear area and therefore, the presence of a cell. The intensity of the Alexa 488 fluorescence in the whole-cell area of the visualised cells was averaged and this value used for further analysis. Alexa 488 fluorescence intensity values, indicating phosphorylation of Ser[375] at the MOPr, had background signal subtracted and were then normalized to both the value obtained for phosphate buffered saline (PBS; basal) and for 100 µM DAMGO.

For Western blots, following agonist treatment, cells were washed three times with ice-cold PBS and lysed in immunoprecipitation buffer (50 mM Tris, pH 7.5, 10 mM EDTA, 150 mM NaCl, 0.5% deoxycholate, 0.1% sodium dodecyl sulphate (SDS), 1% NP-40, 50 mM NaF, 10 mM Glycerol-2-phosphate, 200 µM sodium orthovanadate, 25 mM sodium pyrophosphate and 1 x complete mini protease inhibitor (Roche, Welwyn Garden City, UK). Cell lysates were clarified by centrifugation at 12,000 rpm at 4°C in a microcentrifuge and immunoprecipitated with anti-HA antibody (HA-11; 3 µg per sample; Covance, Maidenhead, UK) and protein G/A-agarose overnight at 4°C. Beads were washed three times with immunoprecipitation buffer and proteins were eluted by the addition of SDS-sample buffer for 3 min at 95°C. Proteins were then resolved by 8% SDS-PAGE and transferred to polyvinylidene difluoride membranes. Membranes were incubated with the anti-pSer[375] polyclonal antibody (1:1,000). Blots were stripped and reprobed with anti-HA antibody (HA-11; 1:1,000). Signal detection was performed by enhanced chemiluminescence.

FRET experiments: These were carried out exactly as described previously (McPherson et al., 2010). Briefly, HEK293 cells co-transfected with MOPr-Yellow Fluorescent Protein (YFP), arrestin-3-Cyan Fluorescent Protein (CFP) and G protein-coupled receptor kinase 2 (GRK2; this increased the agonist-induced FRET signal obtained) were plated out on poly-l-lysine-coated glass coverslips. Cells were mounted on a Nikon Eclipse TE2000S inverted microscope (Nikon, Kingston, UK) and visualized using an oil immersion 63x lens, a polychrome V for excitation, and a dual emission photometric system (Till Photonics, Gräfelfing, Germany). MOPr agonists were applied using a computer-assisted superfusion system. Fluorescence was measured at 535 ± 15 nm (F_{YFP}) and 480 ± 20 nm (F_{CFP}) upon excitation at 436 ± 10 nm. Signals detected by avalanche photodiodes were digitized using an analog/digital converter (Digidata 1322A, Axon Instruments, Union City, CA) and stored on PC using Axoscope 9.2 software (Axon Instruments). FRET was calculated as the ratio F_{YFP}/F_{CFP}. Off-line analysis of the FRET (F_{YFP}/F_{CFP}) data was carried out to determine the kinetics and the extent of the MOPr-YFP and Arrestin3-CFP interaction induced by different agonists.

Cell surface receptor loss: This was assessed by ELISA, as described previously (McPherson et al., 2010). Briefly, HEK293 cells stably expressing HA-tagged MOPr were seeded into 24-well tissue culture dishes coated with 0.1 mg/ml poly-L-lysine for 24 h prior to experimentation. For time course experiments cells were washed and then challenged with DMEM containing opioid agonist for 0-30 min at 37°C. Reactions were terminated by fixing the cells with 3.7% formaldehyde. Cells were then incubated with primary antibody (anti-HA-11, 1:1,000) for 1 h at room temperature. For investigations of the agonist concentration-dependency of internalization, cells were prelabelled with primary antibody at 4°C for 1 h prior to incubation with the agonists for 30 min at 37°C. Cells were then incubated with secondary antibody (goat anti-mouse conjugated with alkaline phosphatase, 1:1,000; Sigma), and a colorimetric alkaline phosphatase

substrate (Bio-Rad Laboratories, Hemel Hempstead, UK) added with samples being assayed at 405 nm in a microplate reader. Changes in surface receptor expression were subsequently determined by normalizing data from each treatment group to corresponding control surface receptor levels determined from cells not exposed to opioid agonist, and expressed as either % surface receptor expression or cell surface loss (as % of no drug control), depending on the primary antibody labelling method used, with the background signal from HEK293 cells subtracted from all receptor-transfected values. All experiments were performed in triplicate.

Data analysis and statistics: All data were analysed using GraphPad Prism. Agonist concentration-response data from LC neurons was first fitted to sigmoid curves with variable slope, with the bottom of the curve in each case constrained to zero, in order to obtain agonist EC_{50} and E_{max} values and for graphical representation of the data. Parameters from this fitting were then also used as initial values for fitting the concentration-response data to the operational model of pharmacological agonism (Black and Leff 1983; see also McPherson et al., 2010; Bailey et al., 2009):

$$E = E_m \tau^n [A]^n / (K_a + [A])^n + \tau^n [A]^n$$

where the response E is expressed in terms of the molar concentration of agonist A, the theoretical maximal effect E_m (greater than that which can be functionally attained; Black and Leff, 1983), the dissociation constant K_a, the transducer ratio τ, and *n*, which is the slope of the curve (NB *n* in this equation is not the same as the Hill slope, although the values can be similar). E_m and *n* are intrinsic properties of the receptor/cell and are independent of the agonist used, whereas τ depends on the cell, receptor function and agonist used. For each pair of curves (i.e. concentration-response curves for DAMGO, etorphine and endomorphin-2 in the presence or absence of 30 nM β-funaltrexamine), values of E_m, K_a and *n* (shared for the paired curves for each agonist) and τ were determined.

MOL #78659

For graphical representation of Ser^{375} phosphorylation, concentration-response data were fitted to sigmoid curves with variable slope, with the bottom of the curve in each case constrained to zero. Parameters from this fitting were then also used as initial values for fitting the concentration-response data to the operational model of pharmacological agonism (see above). For operational model fitting, constrained parameters were E_m shared and <101, n shared and <2.0, and K_a values being those determined previously (McPherson et al., 2010), which were DAMGO, 228 nM; etorphine, 3.5 nM; endomorphin-2, 283 nM; and morphine, 250 nM.

Ser^{375} phosphorylation data were also analysed for efficacy values by the method described previously (Ehlert 1985):

$$e = (\text{Emax}_{agonist}/ \text{Emax}_{full\ agonist}) \times \{(K_{a\ agonist}/ \text{EC}_{50\ agonist})+1\} \times (0.5)$$

where e is the efficacy of the test agonist, and $\text{Emax}_{agonist}/\text{Emax}_{full\ agonist}$ are the relative maximum response values of the test agonist and an agonist giving a full response, whilst K_a and EC_{50} are the equilibrium dissociation constant and EC_{50}, respectively, of the test agonist. The efficacy values for agonist-induced cell surface loss were also determined using this method.

For occupancy-response relationships, data from McPherson et al., 2010 were reanalysed to calculate fractional receptor occupancy at each concentration of agonist used in [^{35}S]GTPγS or arrestin-3 recruitment assays. The fractional receptor occupancy was calculated using the expression $p=[D]/K_a+[D]$ where p is the fractional receptor occupancy (between 0 and 1), [D] is the agonist concentration, and K_a is the equilibrium dissociation constant, the value of which was previously determined in membranes of these cells (McPherson et al., 2010).

For desensitization in LC neurons, the desensitization phase (up to 10 min) from individual experiments were combined and fitted to a one phase exponential decay model to obtain values of $t_{0.5}$ and rate constant k (min^{-1}) of decay, as well as maximum desensitization (plateau level). For analysis of FRET data, the $t_{0.5}$ of the MOPr-YFP/Arrestin3-CFP interaction

11

was obtained by fitting the data from the time points in which the agonist had been applied to a one-phase exponential association model. The extent of the agonist-induced MOPr-YFP and Arrestin3-CFP interaction was calculated as the peak of the interaction and was normalized to the interaction induced by the subsequent application of 10 µM DAMGO.

For ligand bias calculations, the method described by Rajagopal et al (2011) was employed using data previously generated (McPherson et al., 2010). For each agonist with either G protein activation or arrestin-3 recruitment, the "effective signalling" (σ_{lig}) was calculated, where $\sigma_{lig} = \log(\tau_{lig}/\tau_{ref})$. τ_{lig} is the operational efficacy of a ligand for a particular signalling pathway, and τ_{ref} is the operational efficacy for the reference agonist (assumed to be unbiased) for that pathway. In this case the reference ligand was Leu-enkephalin (see Fig 3 of McPherson et al., 2010). The bias factor (β_{lig}) for a particular ligand is then calculated as follows:

$$\beta_{lig} = (\sigma_{lig}^{path1} - \sigma_{lig}^{path2})/\sqrt{2}$$

Statistical differences were determined where appropriate by Student's t test, by one-sample t-test or when comparing different models by F test (selecting the simpler model unless the extra sum-of-squares F test has a $p<0.05$), using GraphPad Prism.

Results

Relative operational efficacy of agonists at native MOPr in mature neurons.

Previously we reported that in HEK293 cells stably expressing MOPr, endomorphin-1 and -2 may be biased towards arrestin recruitment over G protein coupling (McPherson et al., 2010). To investigate whether endomorphins show bias at endogenous MOPrs in mature neurons, we first needed a reliable measure of MOPr agonist efficacy for a G protein-mediated response in LC neurons. We therefore compared the ability of several MOPr agonists to activate inwardly rectifying K^+ channel current (GIRK) in individual rat LC neurons. We constructed concentration-response curves for endomorphin-2, DAMGO, and etorphine, before and after exposure of the brain slices to the irreversible MOPr antagonist β-funaltrexamine (β-FNA; 30 nM, 30 min). In the absence of β-FNA all three agonists produced the same maximum response, indicating that for this response in this tissue, endomorphin-2 is a full agonist (Fig. 1). Pretreatment with β-FNA shifted the agonist-concentration curve for each of these agonists to the right and depressed the maximum response (Fig. 1). The calculated mean ± SEM values for the sigmoid curve fitting are listed in Supplemental Information Table S1.

The curves for each agonist in the absence and presence of β-FNA were then fitted to the equation describing the operational model of pharmacological agonism (Black and Leff, 1983; see Materials and Methods), and values of operational efficacy (τ) obtained. Relative efficacy values are given in Table 1 and calculated mean ± SEM values are listed in Supplemental Information Table S2. In a previous study we obtained a τ value of 1.6 for morphine in LC neurons (Bailey et al., 2009). We and others have previously reported that for morphine the maximum response is lower than that for the other agonists (Bailey et al., 2009; Osborne and Williams 1995), confirming that it is a partial agonist and therefore must have lower efficacy than the other three agonists for this response. The rank order of τ values (see Table 1) obtained from LC neurons (DAMGO> etorphine>> endomorphin-2> morphine) was

13

similar to that previously obtained with these agonists for GTPγS binding in HEK293 cells (McPherson et al., 2010; Table 1), indicating that the relative operational efficacy of G protein-dependent signalling for these agonists is independent of the tissue in which the MOPr is expressed. These data demonstrate that for MOPr-G protein coupling in both a heterologous cell line and in mature neurons, endomorphin-2 has much lower efficacy than DAMGO.

Rate and extent of agonist-induced desensitization of MOPr activated K$^+$ current in LC neurons.

We next assessed the ability of the MOPr agonists to induce acute desensitization of the GIRK current in LC neurons (Fig. 2). A receptor-saturating concentration of each agonist was applied for 10 min and the GIRK current recorded. Representative traces for each agonist are shown in Fig. 2. It can be seen that DAMGO, etorphine and endomorphin-2 induced extensive, rapid desensitization of the GIRK current, whilst morphine induced less desensitization over the same time period. The desensitization phase for each agonist was fitted to a single exponential decay model to determine the rate of desensitization and the maximum amount of desensitization. The data are shown in Fig. 2 and Table 2. The fastest rate of desensitization was for endomorphin-2 (F test, $p<0.0001$), with the order from faster to slower decay rate constant k (min^{-1}) being: endomorphin-2 (0.440) > DAMGO (0.233) > morphine (0.205) > etorphine (0.137). The ability of a number of other MOPr agonists to induce acute desensitization in LC was examined, but none induced faster desensitization than endomorphin-2 (Supplemental Fig. S1). These data indicate that in rat brain neurons the ability of endomorphin-2 to induce rapid desensitization is much greater than would be predicted from its efficacy for GIRK activation.

Agonist-induced phosphorylation of MOPr at Ser^{375}.

MOPr agonists induce phosphorylation at Ser^{375} in the COOH terminus of the receptor, and an antiphosphoreceptor antibody has been developed to identify this phosphorylation event (Schulz et al., 2004). To facilitate measurement of agonist-induced MOPr phosphorylation at Ser^{375}, automated imaging of permeabilised HEK293 cells was undertaken (Fig. 3A). Initial experiments indicated that this Ser^{375} phosphorylation was mediated in part by GRK2, was independent of PKC activation, and partly depended upon coupling to G proteins (Supplemental Fig. S2). Concentration-response curves for phosphorylation of Ser^{375} in response to 10 min of agonist stimulation were constructed. Whilst DAMGO, endomorphin-2 and etorphine appeared to be full agonists in this assay, morphine was a partial agonist (Fig. 3B; see Supplemental Information Table S3 for parameters of fitting data to sigmoid curves). Etorphine was the most potent agonist followed by DAMGO and endomorphin-2 and then morphine. These agonist effects were also confirmed by Western blotting of MOPr immunoprecipitated from HEK293 cells (Fig. 3C). Concentration-response data obtained from the automated imaging were then subjected to operational analysis, using the binding constants for MOPr in HEK293 cells determined in our previous study (McPherson et al., 2010). Relative efficacy values are given in Table 1 and calculated mean ± SEM values are listed in Supplemental Information Table S4. They indicate that, unlike the results from G protein coupling, the operational efficacy of endomorphin-2 for phosphorylation of Ser^{375} in MOPr was similar to that of etorphine and almost as high as that of DAMGO. On the other hand the operational efficacy for morphine remained low in this assay. Because the operational analysis of these data produced τ values with large standard errors (see Supplemental Information Table S4), as an alternative approach to determine relative efficacy in this assay, the data were analysed by the method of Ehlert which uses a combination of EC$_{50}$, maximum response and binding constant (Ehlert 1985; for details see Materials and Methods) to obtain a measure of efficacy (e). This produced a similar rank order of relative efficacy (Table 1) as the operational analysis. Thus, whichever method is used

to determine relative efficacy from these data, the efficacy of endomorphin-2 for Ser^{375} phosphorylation is close to that of DAMGO, even though the latter has a much higher efficacy for G protein activation.

Agonist-induced interaction of MOPr with arrestin-3.

We employed FRET to assess the MOPr/arrestin-3 interaction in intact cells following agonist application. HEK293 cells were transiently transfected with MOPr-YFP and arrestin-3-CFP; 48 h later, FRET was monitored for 3-5 min after the addition of DAMGO (10 μM), etorphine (10 μM), endomorphin-2 (10 μM) or morphine (30 μM). With the exception of etorphine which did not wash out, in each case, DAMGO (10 μM) was added after the first drug had been washed out to obtain a relative measure of maximum response (Fig 4A). Analysis of agonist-induced FRET showed that the $t_{0.5}$ of the MOPr/arrestin-3 association-induced FRET was relatively low for DAMGO and endomorphin-2, and much higher for morphine (Fig. 4B). Furthermore DAMGO and endomorphin-2 produced rapid increases in the FRET ratio that were of similar maximum amplitudes, whilst morphine produced a smaller increase in the FRET ratio than the other agonists (Fig. 4C).

Agonist–induced cell surface loss of MOPr.

The ability of DAMGO, etorphine, endomorphin-2 and morphine to induce loss of cell surface MOPr was assessed by ELISA. Both the agonist concentration- and time-dependency of cell surface loss was assessed (Fig. 5). The agonist concentration response curves indicated that etorphine was the most potent agonist followed by DAMGO, then morphine and endomorphin-2. Receptor saturating concentrations of DAMGO, etorphine and endomorphin-2 applied for 30 min each induced >25% loss of cell surface MOPr (Fig. 5B); a saturating concentration of morphine induced less extensive loss of MOPr (<15%). The parameters for fitting the concentration-response data to sigmoidal curves are shown in Supplemental

Information Table S5. It was not possible to fit the data in Fig. 5A using the operational model, even with a range of constraints, so the relative efficacies were calculated by the method of Ehlert (1985). In this analysis (Table 1), the rank order of relative efficacy values (e) was DAMGO > etorphine = endomorphin-2 > morphine. Together these results show that even though endomorphin-2 has an operational efficacy value for G protein coupling/ K^+ current activation much lower than DAMGO, it is able to induce cell surface loss of MOPr almost the same as that of DAMGO. Furthermore, although in HEK293 cell studies, endomorphin-2 and morphine have comparable low values of operational efficacy for [^{35}S]GTPγS binding, endomorphin-2 induces more extensive cell surface loss of MOPr than morphine.

Comparison of agonist efficacy values for multiple signalling outputs.

To compare relative efficacy values from multiple signalling outputs, efficacy values for each response analysed in this study are presented as a bar graph (Fig. 6), with in each case the efficacy of DAMGO set as 1. This shows that the relative efficacy values of the agonists for GIRK activation and [^{35}S]GTPγS binding (i.e. G protein responses) closely mirror each other, with endomorphin-2 having low efficacy relative to DAMGO. On the other hand the efficacy of endomorphin-2 relative to DAMGO is much higher for phosphorylation of Ser^{375}, arrestin-3 recruitment and cell surface loss. Indeed for Ser^{375} phosphorylation and arrestin-3 recruitment the efficacy of endomorphin-2 is essentially the same as that of DAMGO.

Agonist occupancy-response relationships.

To further examine the agonist-induced responses to the four MOPr agonists, occupancy-response relationships were constructed for MOPr agonists, using previously generated data (McPherson et al., 2010) for [^{35}S]GTPγS binding and arrestin-3 recruitment

17

assays for receptors stably expressed in HEK293 cells (Fig. 7). The transformation of the data

in this way enables an examination of the agonist occupancy-response relationship without the

complication of binding affinity. These results show that in terms of coupling to G protein, the

efficacy order is DAMGO > etorphine > endomorphin-2 = morphine (Fig. 7A; compare agonist

responses at e.g. occupancies of 0.25), whilst for arrestin-3 recruitment it is DAMGO =

etorphine = endomorphin-2 >> morphine (Fig. 7B). It is also clear that the relationship between

fractional receptor occupancy of MOPr and arrestin-3 recruitment is essentially linear,

suggesting a lack of amplification in this response. Of interest, analysis of Ser[375]

phosphorylation and internalization data suggests that the relationship between fractional

receptor occupancy and these outputs is also linear (Supplemental Fig. S3). The occupancy-

response relationship in Fig. 7B might suggest that it is in fact morphine rather than

endomorphin-2 which is unusual, since the arrestin response-fractional receptor occupancy

relationship for morphine lies far apart from those of the other three agonists. To investigate

this, we used previously published data to construct occupancy-response relationships for some

other agonists which had similar operational efficacies in the GTPγS assay (McPherson et al.,

2010), including morphine and endomorphin-2, also oxycodone, 6-monoacetylmorphine (6-

MAM) and morphine-6-glucuronide (M6G). When the occupancy-response relationship for

arrestin-3 recruitment is plotted for this group of agonists, it can be clearly seen that

endomorphin-2 has much higher efficacy than any of the other agonists within this group

(Supplemental Fig. S4). This strongly supports the conclusion that endomorphin-2 is an arrestin-

biased ligand.

Calculation of ligand bias.

In a recent study a method was described to quantify ligand bias (Rajagopal et al.,

2011). In this method, operational efficacy (τ) values are calculated for a series of agonists for

18

two signalling outputs and compared to the τ values for an agonist which is unbiased between the two signalling pathways being assessed (see Materials and Methods). From previous data we concluded that Leu-Enkephalin is an unbiased agonist (see Fig. 3 of McPherson et al., 2010). Using this approach we calculated bias for those MOPr ligands which gave significant responses in the two assays, which enabled us to calculate bias for sixteen of the twenty two ligands investigated in our previous study. Calculation of ligand bias (Fig. 8) indicated that endomorphin-2 was significantly biased towards arrestin-3 recruitment. Although no other ligands displayed statistically significant bias, it is worth noting that endomorphin-1, etorphine and alfentanil displayed a trend towards arrestin-bias, whilst on the other hand DAMGO displayed a trend towards G protein bias.

Discussion

Previous studies on the endomorphins have identified these peptides as selective MOPr agonists with relatively high affinity for the receptor (Zadina et al., 1997). In some cases the endomorphins are reported as partial agonists at MOPr, for example in GTPγS binding assays of spinal cord and thalamus (Hosohata et al., 1998; Narita et al., 1998; Xie et al., 2008; Sim et al., 1998), and in the inhibition of neuronal Ca^{2+} currents (Connor et al., 1999) whereas in others, such as inhibition of contraction of mouse vas deferens the endomorphins can behave as full agonists (Al-Khrasani et al., 2001; Rónai et al., 2006); such differences are likely to be dependent in part upon receptor reserve in each tissue. In the present study using LC neurons we found endomorphin-2 to be a full agonist for activation of GIRK current. However the receptor reserve for the endomorphin-2 response in LC neurons was less than that for DAMGO and etorphine since limited receptor depletion using a low concentration (30 nM) of β-FNA led to a greater reduction in the maximum response to endomorphin-2 (22% reduction) than for DAMGO (7% reduction) or etorphine (15% reduction), as well as a smaller shift in agonist EC_{50} (2.6-fold for endomorphin-2, 5.6-fold for etorphine and 11.5-fold for DAMGO). In order to quantify the efficacy of endomorphin-2 relative to DAMGO and other MOPr agonists, we used the MOPr inactivation method that we (Bailey et al., 2009) and others (Rónai et al., 2006; Madia et al., 2009) have previously used to determine agonist efficacy. From this analysis we determined that the operational efficacy of endomorphin-2 for activation of GIRK was only 7% of that of DAMGO, with etorphine having an intermediate efficacy. These relative values reflect those obtained for GTPγS binding in membranes of HEK293 stably expressing MOPr, where the efficacy value for endomorphin-2 was 17% of that of DAMGO, with etorphine again being intermediate (McPherson et al., 2010). Since the MOPr-mediated activation of GIRK in LC neurons is a G protein-mediated response, it is perhaps not surprising that the relative efficacies in the two assays are similar.

20

Previous studies (Yu et al., 1997; Virk and Williams 2008) suggest that the ability of saturating concentrations of MOPr agonists to induce acute (0-10 min) desensitization is agonist efficacy-dependent. On this basis endomorphin-2 would be predicted to induce relatively little desensitization of MOPr-mediated GIRK activation during this relatively short period of agonist exposure, because of its lower efficacy for this effect. However, endomorphin-2-induced desensitization was as extensive, and occurred more rapidly than that induced by DAMGO. On the other hand, the desensitization induced by morphine and etorphine was slower than that by DAMGO and was in line with efficacy values determined in this study for LC neurons and for [^{35}S]GTPγS binding assays in HEK293 cells (McPherson et al., 2010). The acute desensitization induced by endomorphin-2 may in part be due to the ability of this ligand to induce efficient arrestin recruitment to MOPr, leading to extensive uncoupling of receptor and G protein. However, this cannot be the complete explanation, since the efficacy of endomorphin-2 for arrestin-3 recruitment in HEK293 cells is the same as that of DAMGO, and indeed etorphine (McPherson et al., 2010), yet acute desensitization is faster for endomorphin-2. One possibility is that the low efficacy and consequent small receptor reserve of endomorphin-2 for GIRK activation, coupled with a relatively high efficacy for arrestin recruitment, may make it particularly sensitive to the onset of acute desensitization. On the other hand, DAMGO is an agonist with high efficacy for GIRK activation and consequently large receptor reserve, which would display slower desensitization because although it induces efficient arrestin recruitment to MOPr, the high efficacy for GIRK activation means that a much greater loss of functional receptor would be required than for endomorphin-2, in order to observe significant desensitization of the GIRK response.

Furthermore differences in arrestin-2 vesus arrestin-3 recruitment have not been explored thus far, so it is possible that the profile of arrestin-2 versus arrestin-3 recruitment to the endomorphin-2-occupied MOPr is different from that induced by other agonists, leading to agonist- and arrestin-dependent signalling and regulation which is distinct from other agonists.

Indeed such a scenario has recently been described for arrestin isoform interaction with MOPr in response to DAMGO and morphine (Groer et al., 2011). The precise role of arrestins in MOPr regulation in neurons remains to be fully elucidated. Although in cell lines MOPr desensitization by high efficacy agonists such as DAMGO is arrestin-dependent (Chu et al., 2008), in LC neurons from arrestin-3 KO mice the acute desensitization induced by Met-enkephalin is unaffected (Dang et al., 2011; Quillinan et al., 2011). These recent studies suggest that arrestins indeed play a complex role in MOPr function in neurons, with recovery from acute desensitization being much faster in neurons from arrestin-3 KO mice (Dang et al., 2011; Quillinan et al., 2011). Given that MOPr dephosphorylation can occur at the cell surface (Arttamangkul et al., 2006; Doll et al., 2011), arrestin interaction and internalization could actually reduce the rate of MOPr resensitization, potentially manifesting as an enhanced rate of desensitization, as observed in our LC neuron study.

In further studies we investigated the ability of the agonists DAMGO, etorphine, endomorphin-2 and morphine to (i) induce phosophorylation of Ser^{375} in the COOH-terminus tail of MOPr, (ii) recruit arrestin-3 to MOPr in intact cells by FRET and (iii) induce cell surface loss of MOPr. We reasoned that the ability of endomorphin-2 to effectively recruit arrestin-3 may be because of more rapid or more extensive MOPr phosphorylation at Ser^{375}. Although we (McPherson et al., 2010) and others (Yu et al., 1997) have previously compared the ability of receptor-saturating concentrations of agonist to promote MOPr phosphorylation, in the current study we were able to construct full concentration-response curves for Ser^{375} phosphorylation which allowed estimates of relative agonist efficacy to be made. This revealed that the efficacy of endomorphin-2 to induce Ser^{375}phosphorylation in MOPr was similar to that of DAMGO and much higher than morphine. This, in turn, suggests that it is actually the ability of endomorphin-2 to efficiently promote phosphorylation of MOPr that underlies its ability to recruit arrestin-3 to MOPr and also induce MOPr internalization to a greater extent than morphine. Recent studies indicate that MOPr is phosphorylated on multiple residues in the COOH terminus (Doll et al.,

22

2011; Lau et al., 2011; Kelly et al. unpublished observations), and that the pattern of phosphorylation is agonist-dependent. Ser^{375} is undoubtedly a key residue in terms of arrestin recruitment (Schulz et al., 2004), but other residues may well be important for arrestin recruitment (Lau et al., 2011), and it will be of particular interest to determine the ability of the endomorphins to induce phosphorylation of individual residues in the COOH-terminus of MOPr. Intriguingly, however, this does not explain why endomorphin-2 induces more efficient MOPr phosphorylation than morphine. However, given that biased agonism suggests that different agonists can stabilise distinct active conformations of a GPCR (Kahsai et al., 2011), then it is possible that endomorphin-2 stabilises a conformation of the MOPr that couples relatively poorly to G protein but which is nevertheless readily phosphorylated by kinases, such as GRK2, or possibly kinases distinct from those that phosphorylate the DAMGO- or morphine-occupied MOPr.

The distinction between endomorphin-induced MOPr signalling and trafficking can in fact be deduced from careful analysis of previous studies, where [^{35}S]GTPγS binding assays reveal the endomorphins to have low efficacy values close to those of morphine (Hosohata et al., 1998; Narita et al., 1998; Xie et al., 2008; Sim et al., 1998), yet the endomorphins are able to induce efficient trafficking of MOPr under conditions where morphine is ineffective (Burford et al., 1998; McConalogue et al., 1999; Trafton et al., 2000). The advantages of quantifying efficacy from full concentration-response curves, and of examining occupancy-response relationships, is that such differences are more clearly observed and can be quantified. Indeed, previous studies have often used saturating concentrations of agonist to compare efficacies, which is of limited use when comparing the efficacies of full agonists. In addition, comparison of potencies and maximum responses (intrinsic activity) sometimes does not reveal biased agonism (Molinari et al., 2010). More sophisticated approaches to quantifying ligand bias have recently been proposed (Rajagopal et al., 2011) and the application of one such approach to our

data from HEK293 cells (Fig. 8) identifies the arrestin-bias of endomorphin-2 to be statistically significant .

In conclusion, endomorphin-2 is an arrestin-biased MOPr agonist, and this may be explained by the drug's ability to promote efficient phosphorylation of the receptor. Future studies will be focussed on determining whether the pattern of MOPr phosphorylation induced by endomorphin-2 is different from that of other agonists such as DAMGO and morphine. Endomorphin-related ligands are reported to have a favourable profile in terms of analgesia, and tolerance/dependence and appear to produce less respiratory depression than other agonists (Zadina, unpublished data). It remains to be seen whether or not this profile is due to the behaviour of the endomorphins as arrestin-biased ligands at MOPr.

Authorship Contribution

Participated in research design: EK, GH, CPB, SJM, CAM, EMR, SJC, CK
Conducted experiments: GR, JL, JM, AC
Contributed new reagents or analytical tools: CAM, CK
Performed data analysis: GR, JL, JM, AC, EK, CAM
Wrote or contributed to writing of the Manuscript: EK, GH, CPB, SJM, CAM, EMR, SJC, CK

REFERENCES

Al-Khrasani M, Orosz G, Kocsis L, Farkas V, Magyar A, Lengyel I, Benyhe S, Borsodi A and Rónai AZ (2001) Receptor constants for endomorphin-1 and endomorphin-1-ol indicate differences in efficacy and receptor occupancy. *Eur J Pharmacol* **421**(1):61-67.

Arttamangkul S, Torrecilla M, Kobayashi K, Okano H and Williams JT (2006) Separation of mu-opioid receptor desensitization and internalization: endogenous receptors in primary neuronal cultures. *J Neurosci* **26**(15):4118-4125.

Bailey C, Couch D, Johnson E, Griffiths K, Kelly E and Henderson G (2003) Mu-opioid receptor desensitization in mature rat neurons: lack of interaction between DAMGO and morphine. *J Neurosci* **23**(33):10515-10520.

Bailey C, Llorente J, Gabra B, Smith F, Dewey W, Kelly E and Henderson G (2009) Role of protein kinase C and mu-opioid receptor (MOPr) desensitization in tolerance to morphine in rat locus coeruleus neurons. *Eur J Neurosci* **29**(2):307-318.

Black JW and Leff P (1983) Operational models of pharmacological agonism. *Proc R Soc Lond B Biol Sci* **220**(1219):141-162.

Burford NT, Tolbert LM and Sadee W (1998) Specific G protein activation and mu-opioid receptor internalization caused by morphine, DAMGO and endomorphin I. *Eur J Pharmacol* **342**(1):123-126.

Caunt CJ, Armstrong SP and McArdle CA (2010) Using high-content microscopy to study gonadotrophin-releasing hormone regulation of ERK. *Methods Mol Biol* **661**:507-524.

Chu J, Zheng H, Loh HH and Law PY (2008) Morphine-induced mu-opioid receptor rapid desensitization is independent of receptor phosphorylation and beta-arrestins. *Cell Signal* **20**(9):1616-1624.

Connor M, Schuller A, Pintar JE and Christie MJ (1999) Mu-opioid receptor modulation of calcium channel current in periaqueductal grey neurons from C57B16/J mice and mutant mice lacking MOR-1. *Br J Pharmacol* **126**(7):1553-1558.

Corbett AD, Henderson G, McKnight AT and Paterson SJ (2006) 75 years of opioid research: the exciting but vain quest for the Holy Grail. *Br J Pharmacol* **147 Suppl 1**:S153-162.

Dang VC, Chieng B, Azriel Y and Christie MJ (2011) Cellular morphine tolerance produced by βarrestin-2-dependent impairment of μ-opioid receptor resensitization. *J Neurosci* **31**(19):7122-7130.

Doll C, Konietzko J, Pöll F, Koch T, Höllt V and Schulz S (2011) Agonist-selective patterns of μ-opioid receptor phosphorylation revealed by phosphosite-specific antibodies. *Br J Pharmacol* **164**(2):298-307.

Ehlert FJ (1985) The relationship between muscarinic receptor occupancy and adenylate cyclase inhibition in the rabbit myocardium. *Mol Pharmacol* **28**(5):410-421.

Groer CE, Schmid CL, Jaeger AM and Bohn LM (2011) Agonist-directed interactions with specific beta-arrestins determine mu-opioid receptor trafficking, ubiquitination, and dephosphorylation. *J Biol Chem* **286**(36):31731-31741.

Hosohata K, Burkey TH, Alfaro-Lopez J, Varga E, Hruby VJ, Roeske WR and Yamamura HI (1998) Endomorphin-1 and endomorphin-2 are partial agonists at the human mu-opioid receptor. *Eur J Pharmacol* **346**(1):111-114.

Kahsai AW, Xiao K, Rajagopal S, Ahn S, Shukla AK, Sun J, Oas TG and Lefkowitz RJ (2011) Multiple ligand-specific conformations of the β_2-adrenergic receptor. *Nat Chem Biol* **7**(10):692-700.

Kenakin T (2011) Functional selectivity and biased receptor signaling. *J Pharmacol Exp Ther* **336**(2):296-302.

Lau EK, Trester-Zedlitz M, Trinidad JC, Kotowski SJ, Krutchinsky AN, Burlingame AL and von Zastrow M (2011) Quantitative encoding of the effect of a partial agonist on individual opioid receptors by multisite phosphorylation and threshold detection. *Sci Signal* **4**(185):ra52.

Madia PA, Dighe SV, Sirohi S, Walker EA and Yoburn BC (2009) Dosing protocol and analgesic efficacy determine opioid tolerance in the mouse. *Psychopharmacology (Berl)* **207**(3):413-422.

McConalogue K, Grady EF, Minnis J, Balestra B, Tonini M, Brecha NC, Bunnett NW and Sternini C (1999) Activation and internalization of the mu-opioid receptor by the newly discovered endogenous agonists, endomorphin-1 and endomorphin-2. *Neuroscience* **90**(3):1051-1059.

McPherson J, Rivero G, Baptist M, Llorente J, Al-Sabah S, Krasel C, Dewey W, Bailey C, Rosethorne E, Charlton S, Henderson G and Kelly E (2010) µ-Opioid receptors: correlation of agonist efficacy for signalling with ability to activate internalization. *Mol Pharmacol* **78**(4):756-766.

Molinari P, Vezzi V, Sbraccia M, Grò C, Riitano D, Ambrosio C, Casella I and Costa T (2010) Morphine-like opiates selectively antagonize receptor-arrestin interactions. *J Biol Chem* **285**(17):12522-12535.

Morgan MM and Christie MJ (2011) Analysis of opioid efficacy, tolerance, addiction and dependence from cell culture to human. *Br J Pharmacol* **164**(4):1322-1334.

Narita M, Mizoguchi H, Oji GS, Tseng EL, Suganuma C, Nagase H and Tseng LF (1998) Characterization of endomorphin-1 and -2 on [^{35}S]GTPgammaS binding in the mouse spinal cord. *Eur J Pharmacol* **351**(3):383-387.

North RA and Williams JT (1985) On the potassium conductance increased by opioids in rat locus coeruleus neurones. *J Physiol* **364**:265-280.

Osborne PB and Williams JT (1995) Characterization of acute homologous desensitization of mu-opioid receptor-induced currents in locus coeruleus neurones. *Br J Pharmacol* **115**(6):925-932.

Quillinan N, Lau EK, Virk M, von Zastrow M and Williams JT (2011) Recovery from mu-opioid receptor desensitization after chronic treatment with morphine and methadone. *J Neurosci* **31**(12):4434-4443.

Rajagopal S, Ahn S, Rominger DH, Gowen-MacDonald W, Lam CM, Dewire SM, Violin JD and Lefkowitz RJ (2011) Quantifying ligand bias at seven-transmembrane receptors. *Mol Pharmacol* **80**(3):367-377.

Reiter E, Ahn S, Shukla AK and Lefkowitz RJ (2011) Molecular Mechanism of β-Arrestin-Biased Agonism at Seven-Transmembrane Receptors. *Annu Rev Pharmacol Toxicol*.

Rónai AZ, Al-Khrasani M, Benyhe S, Lengyel I, Kocsis L, Orosz G, Tóth G, Kató E and Tóthfalusi L (2006) Partial and full agonism in endomorphin derivatives: comparison by null and operational model. *Peptides* **27**(6):1507-1513.

Schulz S, Mayer D, Pfeiffer M, Stumm R, Koch T and Höllt V (2004) Morphine induces terminal micro-opioid receptor desensitization by sustained phosphorylation of serine-375. *EMBO J* **23**(16):3282-3289.

Shenoy SK and Lefkowitz RJ (2011) β-Arrestin-mediated receptor trafficking and signal transduction. *Trends Pharmacol Sci* **32**(9):521-533.

Sim LJ, Liu Q, Childers SR and Selley DE (1998) Endomorphin-stimulated [35S]GTPgammaS binding in rat brain: evidence for partial agonist activity at mu-opioid receptors. *J Neurochem* **70**(4):1567-1576.

Terskiy A, Wannemacher KM, Yadav PN, Tsai M, Tian B and Howells RD (2007) Search of the human proteome for endomorphin-1 and endomorphin-2 precursor proteins. *Life Sci* **81**(23-24):1593-1601

Trafton JA, Abbadie C, Marek K and Basbaum AI (2000) Postsynaptic signaling via the [mu]-opioid receptor: responses of dorsal horn neurons to exogenous opioids and noxious stimulation. *J Neurosci* **20**(23):8578-8584.

Virk MS and Williams JT (2008) Agonist-specific regulation of mu-opioid receptor desensitization and recovery from desensitization. *Mol Pharmacol* **73**(4):1301-1308.

Xie H, Woods JH, Traynor JR and Ko MC (2008) The spinal antinociceptive effects of endomorphins in rats: behavioral and G protein functional studies. *Anesth Analg* **106**(6):1873-1881.

Yu Y, Zhang L, Yin X, Sun H, Uhl GR and Wang JB (1997) Mu opioid receptor
   phosphorylation, desensitization, and ligand efficacy. *J Biol Chem* **272**(46):28869-
   28874.

Zadina JE, Hackler L, Ge LJ and Kastin AJ (1997) A potent and selective endogenous
   agonist for the mu-opiate receptor. *Nature* **386**(6624):499-502.

MOL #78659

Footnote

Guadalupe Rivero and Javier Llorente should be considered as joint first authors.

LEGENDS FOR FIGURES

Fig. 1. Concentration-response curves for the activation of the GIRK current in rat LC neurons by DAMGO, etorphine and endomorphin-2. In individual LC neurons, concentration-response curves for **(A)** DAMGO (n= 3-5), **(B)** etorphine (n=3-8) and **(C)** endomorphin-2 (n=3-5) before (filled circles) and after treatment (open circles) with the irreversible MOPr antagonist β-funaltrexamine (β-FNA, 30 nM) for 30 min, normalized to the maximum current induced by noradrenaline (NA, 100 µM) in the same neuron. Each concentration of agonist was applied until the response had reached a steady state (± 2 min). Different concentrations were tested on each neuron to ensure that the responses to higher concentrations of agonist were not attenuated by desensitization. For graphical representation the data were fitted to sigmoidal concentration-response curves with variable slope.

Fig. 2. Rate and extent of desensitization of MOPr-evoked GIRK channel currents in rat LC neurons. (A) Outward potassium current recorded from single LC neurons clamped at -60 mV in response to application of saturating concentrations of DAMGO (10 µM), endomorphin-2 (30 µM), morphine (30 µM) and etorphine (1 µM). Agonists, applied for at least 10 min, induced an outward current that was not sustained for the period of drug application (indicated by the solid bar) but declined (desensitization) to a steady state (plateau). Note that the rate of desensitization to etorphine is slow and needs longer to reach the plateau. The opioid receptor antagonist naloxone (Nlx, 1 µM) was perfused immediately after each agonist to restore the basal level. **(B)** The desensitization phase for each agonist from between 3 and 10 neurons for each agonist was best fitted to a single phase exponential decay model (one and two phase exponential decay models were compared by an F test for each data set). The fastest rate of desensitization observed was for endomorphin-2. Values shown are means ± SEM.

Fig. 3. Image-based quantification of agonist-induced phosphorylation of Ser[375] in MOPr.

HEK293 cells stably expressing HA-tagged MOPr were plated in 96-well plates and exposed to different concentrations of MOPr agonists for 10 min. Cells were then fixed and used for immunocytochemical staining with an anti-pSer[375] antibody and image analysis undertaken as described in Materials and Methods. **(A)** Representative images of the Ser[375] phosphorylated MOPr immunofluorescent signal and the DAPI staining on non-treated cells (PBS), and on cells treated with DAMGO (10 μM), morphine (30 μM) or endomorphin-2 (30 μM) are shown. Cells in mitotic process showed a high non-specific immunofluorescence signal. Scale bar, 30 μm. Results shown are representative of 3-6 independent experiments. **(B)** Concentration-response curves for Ser[375] phosphorylation. Values are means ± SEM of 3-6 independent experiments. **(C)** Western blot of pSer[375] MOPr immunoprecipitated from HEK293 cells using anti-HA antibody and identified with anti-pSer[375] antibody. Note that endomorphin-2 (E2, 30 μM) induced phosphorylation of Ser[375] similar to that induced by DAMGO (D, 10 μM) and much greater than that induced by morphine (M, 30 μM).

Fig. 4. Agonist-induced interaction of MOPr with arrestin-3 as measured by FRET.

HEK293 cells were transiently transfected with MOPr-YFP, GRK2 and arrestin-3-CFP. **(A)** Example of FRET trace for DAMGO (10 μM). An increase in the FRET ratio (measured as $F535/F480$) reflects the interaction between MOPr-YFP and arrestin 3-CFP. **(B)** Half-life ($t_{0.5}$) of MOPr-YFP/ arrestin-3-CFP interaction following addition of 10 μM DAMGO, 30 μM endomorphin-2 or 30 μM morphine. FRET traces were fitted to a single phase exponential to calculate $t_{0.5}$. Values are means ± SEM from at least 3 separate experiments in each case. [**]Value of $t_{0.5}$ for morphine was significantly longer than that for DAMGO or endomorphin-2, P<0.01 Student's t test. **(C)** Extent of agonist-induced FRET. Maximum FRET for each agonist was expressed as a % of that induced by subsequent addition of 10 μM DAMGO. The value for

DAMGO is greater than 100 % since the second DAMGO response was always slightly less than the first (see panel A). Values are means ± SEM from at least 3 separate experiments in each case. [**]Value for morphine was significantly lower than that for DAMGO or endomorphin-2, $P<0.01$ Student's t test.

Fig. 5. Concentration- and time-dependent cell surface loss of MOPr from HEK293 cells stably expressing HA-tagged MOPr. (A) Cells were incubated with different concentrations of agonist for 30 min before determining cell surface MOPr loss by ELISA. Data were fitted to sigmoid curves with variable slope. Values are means ± SEM from 4 separate experiments, each performed in triplicate. **(B)** Cells were incubated with receptor saturating concentrations of agonist (morphine 30 µM; endomorphin-2 30 µM; DAMGO 10 µM; etorphine 1 µM) for up to 30 min to determine time-dependent cell surface loss of MOPr. Values are means ± SEM from 3-5 separate experiments, each performed in triplicate.

Fig. 6. Relative efficacy values for DAMGO, etorphine, endomorphin-2 and morphine for five MOPr signaling outputs. Values refer to efficacy relative to DAMGO, which was set as 1.00 for each output. The values for [^{35}S]GTPγS binding and arrestin-3 recruitment were taken from Table 2 of McPherson et al. (2010). In each case the efficacy values are τ values of operational efficacy, apart from cell surface loss where the values are relative efficacy (e) obtained by the method of Ehlert (1985). Finally, the τ value for morphine in the GIRK assay was obtained from Bailey et al. (2009). Actual values of efficacy for DAMGO in each assay are given in Table 1.

Fig. 7. Fractional receptor occupancy-response relationships for MOPr agonists. Previously published (McPherson et al., 2010) concentration-response data for agonist-induced

[^{35}S]-GTPγS binding and arrestin-3 recruitment was used to determine the occupancy-response relationship for MOPr agonists. Fractional receptor occupancy at each concentration of agonist was calculated as described in Materials and Methods. **(A)** Relationship between [^{35}S]GTPγS binding and fractional receptor occupancy for DAMGO, etorphine, morphine and endomorphin-2. Data were fitted to a one site binding (hyperbola) in Graphpad Prism, r^2 values for each was >0.964. Data points represent the mean response at each level of occupancy. **(B)** Relationship between arrestin-3 recruitment and fractional receptor occupancy for DAMGO, etorphine, morphine and endomorphin-2. Data were fitted by linear regression as this gave a better fit than to a one site binding (hyperbola) model. Data points represent the mean response at each level of occupancy.

Fig. 8. Calculation of ligand bias at MOPr. The bias factor for sixteen MOPr ligands was calculated as described in Materials and Methods, using data for ligand-induced [^{35}S]GTPγS binding and arrestin-3 recruitment previously generated in HEK293 cells stably expressing MOPr (McPherson et al., 2010). Leu-enkephalin was selected as the reference, unbiased ligand on the basis of its position when operational efficacy values for the two signalling outputs were plotted (see Fig. 3 of "McPherson et al., 2010"). For each agonist with either G protein activation or arrestin-3 recruitment, the "effective signalling" (σ_{lig}) was calculated, where $\sigma_{lig} = \log(\tau_{lig}/\tau_{ref})$, and the bias factor ($\beta_{lig}$) for a particular ligand was then calculated using $\beta_{lig} = (\sigma_{lig}^{path1} - \sigma_{lig}^{path2})/\sqrt{2}$. A one sample two tailed t test was used to determine whether the degree of bias was statistically different from zero. Endomorphin-2 displayed a statistically significant level of bias ($p < 0.05$).

Table 1. Comparison of relative efficacy values for different agonist-induced responses at MOPr

Assay	Relative efficacy values; DAMGO set to 1.00 in each case (value in brackets gives actual τ or e value for DAMGO in that assay)			
	DAMGO	**Etorphine**	**Endomorphin-2**	**Morphine**
GIRK current activation (τ) *LC neurons*	1.00 (100.5)	0.43	0.07	0.02[††]
GTPγS binding (τ) *HEK293 cells*	1.00[†] (28.5)	0.40[†]	0.18[†]	0.18[†]
Ser^{375} phosphorylation (τ) *HEK293 cells*	1.00 (1.99)	0.92	0.92	0.44
Ser^{375} phosphorylation (e) *HEK293 cells*	1.00 (0.66)	0.83	0.97	0.52
Arrestin-3 recruitment (τ) *HEK293 cells*	1.00[†] (0.82)	0.98[†]	1.02[†]	0.26[†]
Cell surface receptor loss (e) *HEK293 cells*	1.00 (0.71)	0.70	0.68	0.34

Values refer either to relative operational efficacy (τ) calculated using the operational model or to relative efficacy (e) calculated according to the method (Ehlert et al., 1985) described in the Materials and Methods. In each case the actual value of τ or e for DAMGO in each assay is shown in brackets. [†]Values taken from McPherson et al. (2010). [††]Value calculated from data reported by Bailey et al. (2009).

Table 2. Agonist-induced desensitization of MOPr-activated GIRK current in LC neurons.

Agonist	$t_{0.5}$ for desensitization (min) [confidence intervals]	Extent of desensitization; % [confidence intervals]
Endomorphin-2 (30 μM)	1.58 [1.52-1.64]	47.9 [47.4-48.4]
DAMGO (10 μM)	2.98 [2.76-3.23]	52.7 [51.1-54.3]
Etorphine (1 μM)	5.04 [4.10 - 6.55]	54.6 [47.4-61.8]
Morphine (30 μM)	3.38 [3.16-3.63]	30.2 [29.1-31.3]

The desensitization phase for a saturating concentration of each agonist from a number of experiments as shown in Fig. 2B were fitted to a single phase exponential decay model, to obtain values of $t_{0.5}$ and the extent of desensitization (plateau). Values shown are means with confidence intervals in brackets.
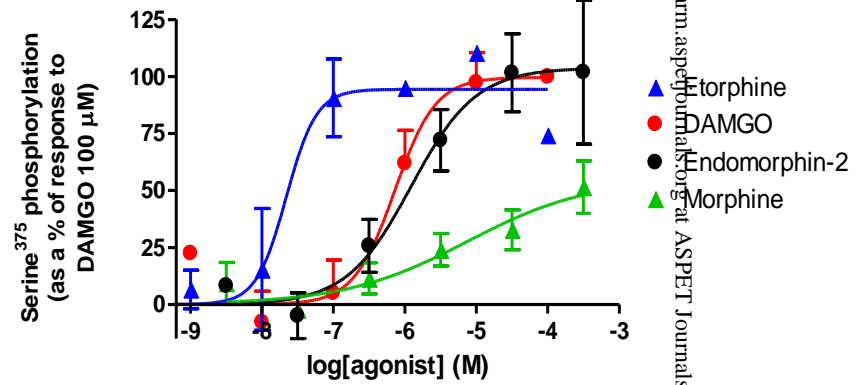
Figure 1

A

B

C

Figure 2

Figure 3

A

	pSer375	DAPI
PBS		
DAMGO 10 µM		
Morphine 30 µM		
Endomorphin-2 30 µM		

B

- ▲ Etorphine
- ● DAMGO
- ● Endomorphin-2
- ▲ Morphine

C

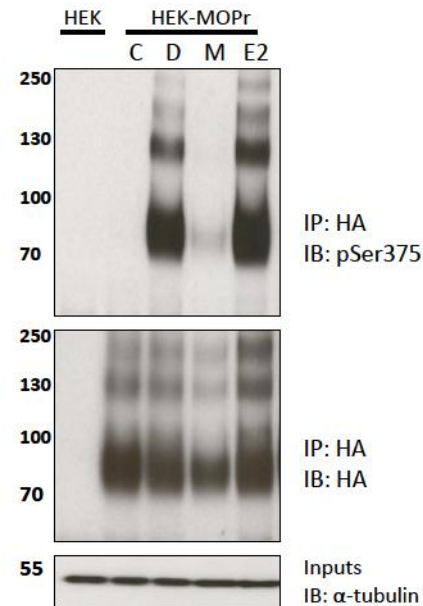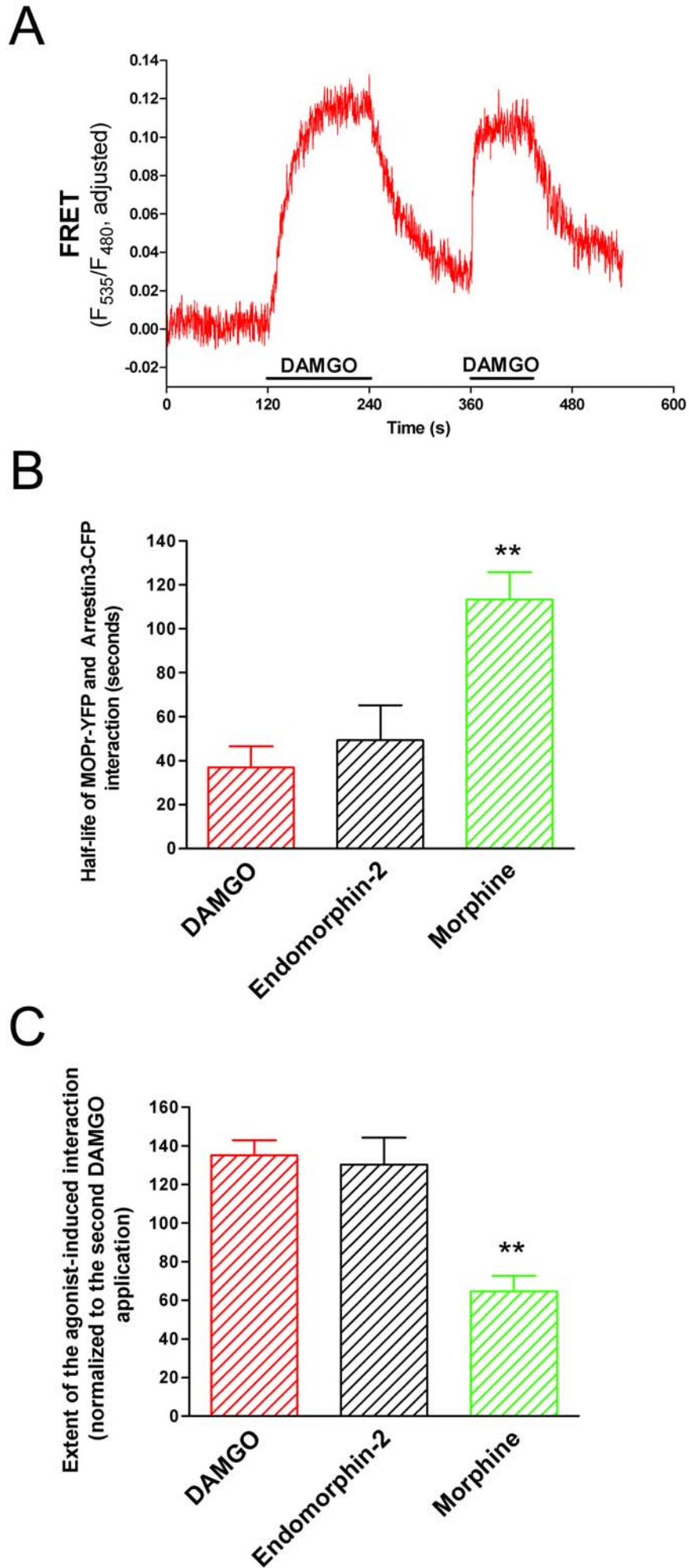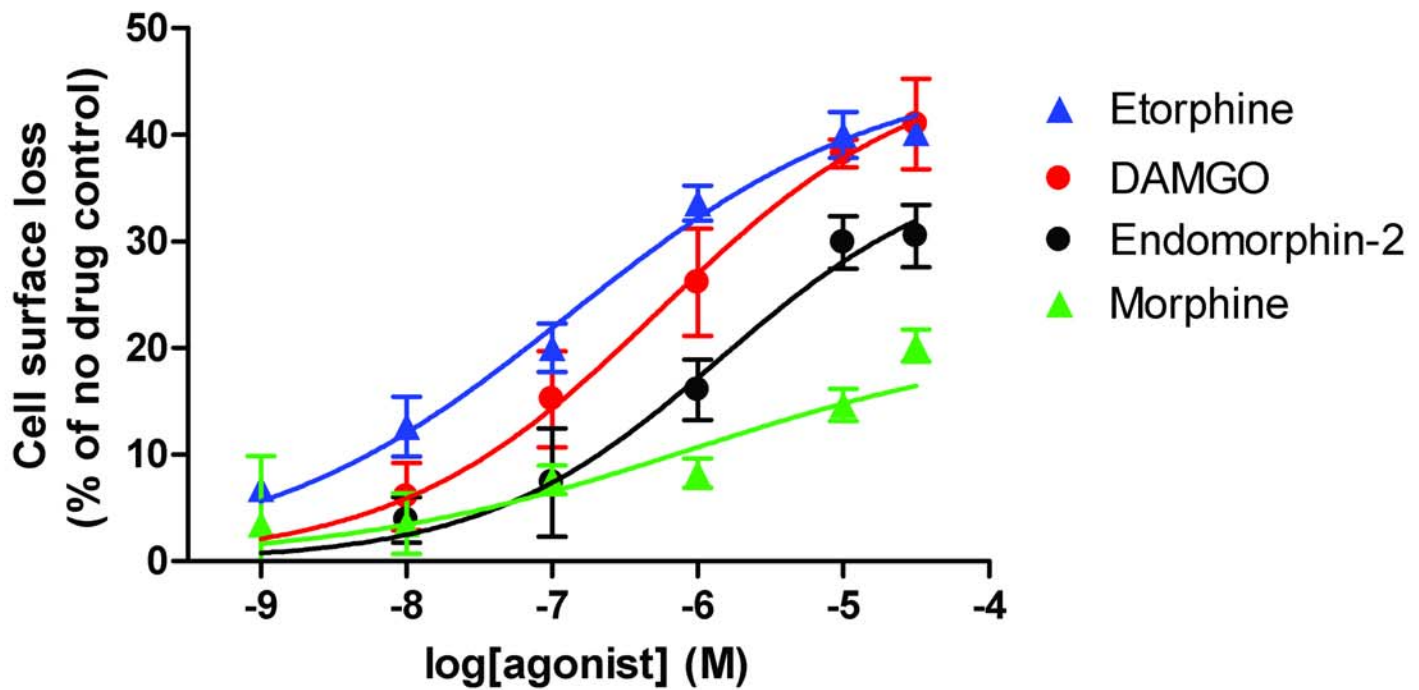HEK   HEK-MOPr
C   D   M   E2

IP: HA
IB: pSer375

IP: HA
IB: HA

Inputs
IB: α-tubulin

Figure 4

Figure 5

Figure 6

Figure 7

A

GTPγS assay

B

Arrestin assay

Figure 8

Legend:
- DAMGO (1)
- Methadone (2)
- Met-enkephalin (3)
- Leu-enkephalin (4)
- Morphine (5)
- Oxycodone (6)
- M6G (7)
- Levorphanol (8)
- Normorphine (9)
- 6-MAM (10)
- Fentanyl (11)
- Norbuprenorphine (12)
- Alfentanil (13)
- Etorphine (14)
- Endomorphin-1 (15)
- Endomorphin-2 (16)